Energy & Environmental Science

ROYAL SOCIETY OF CHEMISTRY

PAPER

View Article Online
View Journal | View Issue

Cite this: *Energy Environ. Sci.*, 2020, **13**, 2191

Thermally regenerative copper nanoslurry flow batteries for heat-to-power conversion with low-grade thermal energy†

Sunny Maye, [a] Hubert H. Girault [a] and Pekka Peljo *[ab]

Low-grade heat (below 200 °C) is available in vast quantities from industry, or from standard roof-top solar thermal collectors. However, the production of electric power from these heat sources is challenging with existing technologies. Thermally regenerative batteries allow both the conversion and the storage of thermal energy into electric power, but they suffer from low operation voltages and low output power. Here, we propose a thermally regenerative nanoslurry flow battery based on copper complexation with acetonitrile in non-aqueous solutions operating at voltages above 1 V. The Cu(I) complex can be destabilized by the removal of acetonitrile by distillation, leading to the production of solid copper nanoparticles and Cu(II) in solution, thereby charging the battery. We demonstrate the electricity production at average power densities of 90 W m^{-2} and peak-power densities up to 150 W m^{-2}, and estimate the theoretical efficiency of the full system at 2%. The results demonstrate a proof-of-concept for harvesting and storage of electricity from low-quality heat.

Received 19th May 2020,
Accepted 9th June 2020

DOI: 10.1039/d0ee01590c

rsc.li/ees

Broader context

Low-grade thermal energy (<200 °C) generated by industry, but also increasingly available from geothermal energy sources and rooftop solar thermal collectors, is an enormous underutilized resource. For example, as much as 20 to 50% of the energy consumed in the industrial manufacturing processes is lost as waste heat. Although waste heat recovery offers significant energy savings and improved energy efficiency, it is still not industrially exploited. This shows that the technical challenges for utilizing this energy are higher than for converting wind or solar energy into electricity. In this work, we have doubled the cell voltage of a thermally regenerative flow battery to 1.2 V. Although thermo-electrochemical systems have been demonstrated earlier, achieving a cell voltage larger than 1 V opens the way to practical electrochemical heat recovery systems. As this work envisages a major leap forward in terms of theoretical thermal conversion efficiency, cell voltage, and energy storage density, these improvements could make this technology industrially relevant.

Introduction

Environmental concerns about the use of natural resources drive us to improve the energy efficiency of existing processes. In this context, the large availability of low-grade heat (temperatures < 200 °C) mainly from industry, but also from geothermal sources and solar thermal collectors, has drawn increasing attention for heat-to-power generation.[1–5] Thermoelectric devices (solid-state semiconductor-based systems) have been extensively investigated for these purposes, but remain expensive and require an additional battery to realize energy storage.[6–8] While conventional approaches to heat-to-power conversion, such as steam turbines, are limited to relatively high cold temperatures (above 100 °C at 1 atm pressure) to avoid condensation of water, the organic Rankine cycle or the Kalina cycle circumvent this problem by replacing water with lower boiling point organic solvents or ammonia, but such systems require large scale installations and cannot store energy.[9–13]

Thermoelectrochemical systems for heat-to-power conversion have been reviewed recently.[5,14,15] Liquid-based thermoelectric systems, where a cell voltage is produced by a temperature gradient between the two electrodes,[16,17] and salinity gradient energy systems, utilizing different salt concentrations obtained by evaporation to generate cell voltages,[18,19] are only able to produce modest cell voltages (<300 mV) and output powers.

[a] *Laboratoire d'Électrochimie Physique et Analytique, École Polytechnique Fédérale de Lausanne, EPFL Valais Wallis, Rue de l'Industrie 17, Case Postale 440, CH-1951 Sion, Switzerland*

[b] *Research group of Physical Electrochemistry and Electrochemical Physics, Department of Chemistry and Materials Science, Aalto University, PO Box 16100, FI-00076 Aalto, Finland. E-mail: pekka.peljo@aalto.fi*

† Electronic supplementary information (ESI) available: Synthesis and characterization of Cu(I) salts, viscosity of acetonitrile–propylene carbonate mixtures, electrochemistry of copper, flow battery experiments, thermal regeneration and differential scanning calorimeter measurements. See DOI: 10.1039/d0ee01590c

On the other hand, higher cell voltages can be achieved with thermally regenerative batteries, where thermal reactions induce a chemical reaction to charge the battery. Most thermally regenerative batteries are based on copper[20–22] or silver[23] complexation with ammonia or acetonitrile[24,25] in aqueous solutions. The removal or addition of the complexing agent is used to change or even inverse the cell voltage,[20–22] or to induce disproportionation of a Cu(I) complex to produce Cu and Cu(II) as described below.[24,25] Cu and Cu(II) can then be discharged in a battery to produce electricity. The advantage of these systems is that in addition to heat-to-power conversion, they are also able to store energy.[24] However, almost all the concepts proposed in the literature show cell voltages below *ca.* 0.65 V, resulting in low output power. One exception is a Zn and Cu based system using ammonia to change the voltage of the positive Cu-electrode, enabling operation at high power densities but low thermal efficiencies of $<1\%$.[26]

These recent reports show that exploitation of low-temperature heat sources by means of unconventional technologies is attracting significant interest from the scientific community. The main difficulty has been to reach a reasonable efficiency, of the order of 10%. Currently, only one technique reaches this goal (demonstrating efficiency of 8%)[27–30] while the others are limited to 1% or less.[5]

One approach to increase the cell voltage is to remove water. Indeed, an all-copper battery in water-free acetonitrile has a cell voltage of 1.3 V[31] in comparison to an aqueous system cell voltage of 0.62 V.[24] It is important to note that the all-copper battery in non-aqueous acetonitrile reported by Kratochvil & Betty[31] cannot be charged with heat, as removal of all the solvent would result in a mixture of solid copper powder and Cu(II) salt precipitate. Therefore, a higher boiling point co-solvent such as water[24] or propylene carbonate utilized in this work is required to realize thermal charging. As acetonitrile forms an azeotrope with water (distillation results in removal of both water and acetonitrile),[25] replacement of water with another high boiling point co-solvent allows reduction in the energy demand for the thermal regeneration step. While a thermally regenerative copper battery employing 30% aqueous acetonitrile solution has a maximum theoretical efficiency of *ca.* 6% mainly due to the low cell voltage and the energy demand to evaporate water, the non-aqueous systems described here show much higher theoretical efficiencies of up to 13%.

In this work, we demonstrate unprecedented cell voltage and high output power for a thermo-electrochemical battery, by utilizing a copper-acetonitrile system with propylene carbonate as a co-solvent due to its high boiling point (242 °C) and stability. The co-solvent is essential to solubilize the Cu(II) salt, allowing separation of solid copper from the Cu(II) electrolyte. We characterize all the thermodynamic parameters of the system to evaluate the theoretical full cycle efficiency, and demonstrate the heat-to-power production and storage with this system.

Here, we demonstrate that the theoretical efficiency can reach up to 2%, with a volumetric energy density of 2.6 W h L^{-1}, and show how these numbers can be significantly improved. These values are higher than reported previously (0.5% and 0.65 W h L^{-1})[20] whilst keeping a similar power density. This significant enhancement in comparison with previous studies on thermally regenerable systems is obtained because of increased cell voltage, from 0.5 V[20] up to 1.2 V in this work.

The remaining challenge of this type of system has been the question of how to reintroduce the heat-charged electrolytes into the electrochemical cell. In this work we solve this issue by utilizing nanoslurry based copper electrolytes. Slurry-based flow batteries have been demonstrated before, but they require careful control of the particle size.[32–34] In this work, nanosized copper slurry is used to promote nucleation of the copper recovered by the thermal regeneration. This allows separation of copper from the thermally regenerated solution by for example centrifugation. Addition of acetonitrile into the copper nanoparticles allows recirculation of the copper through the electrochemical cell as a slurry without compromising the power density or energy storage capacity, as demonstrated in this work.

Experimental

Chemicals

All solvents and chemicals were used as received without further purification and were stored in a glove box under nitrogen. The solvents were acetonitrile (CH_3CN, extra dry over molecular sieves, 99.9%, Acros) and propylene carbonate ($C_4H_6O_3$, anhydrous, 99.7%, Sigma-Aldrich). The supporting electrolytes were tetraethylammonuim tetrafluoroborate ($TEABF_4$, 99%, ABCR) or lithium hexafluorophosphate ($LiPF_6$, Battery Grade, Fluorochem). Tetrakis(acetonitrile)copper(I) hexafluorophosphate ($[Cu(CH_3CN)_4]PF_6$, 98%, ABCR) was used as received as a redox active molecule in the RFB. The electroactive species tetrakis(acetonitrile)copper(I) tetrafluoroborate was either commercial, ($[Cu(CH_3CN)_4]BF_4$, >98%, TCi), or prepared by comproportionation reactions. The reducing ability of metallic Cu on Cu^{2+} has been known since 1923, when Morgan used this method for the preparation of cuprous chloride or bromide-mono(acetonitrile) complexes.[35] Therefore the synthesis of Cu^+ can be easily made in acetonitrile by comproportionation (*cf.* ESI†).[36–38] Regarding the Cu particles synthesis by the cathodic corrosion method, the Cu wires (dia. 0.2 mm and 1 mm, purity 99.9%, Advent) were placed in the aqueous bath (MiliQ water, 18.2 MΩ cm) of PVP (polyvinylpyrrolidone, MW ≈ 10 000, Sigma-Aldrich) and sulphuric acid (H_2SO_4, 95–97% for analysis, Merk).

Cu particle synthesis

The production of the Cu particles for the slurry electrode is carried out *via* the cathodic corrosion method, which is inspired from Koper *et al.*[39,40] An automatized set-up for Cu corrosion is developed for a constant production. The motorized equipment drives a thin Cu wire (dia. 0.2 mm, purity 99.9%, Advent) in an aqueous acidic bath (1 M H_2SO_4) with a stabilizing agent (1 wt% PVP). The speed of the falling wire can be tuned

between 2 and 8 mm min^{-1}. The corrosion of the Cu wire is generated when the electrified wire is introduced in the conductive bath solution, in which a second Cu wire is placed as a type of counter electrode. The technical details of this setup are given in the ESI.† The electrical circuit generates a square-wave signal with a frequency of 100 Hz (programmable function generator, HM8 150, Rohde & Schwarz Hameg) and with a polarization from a DC current switching between ±10 V (DC power supply, RND 320-K3005D, RND Lab). The fast change of polarization is the driving force for the electrical corrosion of the thin wire when it is immerged in the bath. To remove water from the Cu particles, the bath for corrosion is centrifuged and the particles washed several times with ACN, before being finally dried under vacuum.

Electrochemical analysis

Electrochemical analyses were obtained with a Metrohm Autolab potentiostat. All experiments were performed under an anaerobic atmosphere with a flow of nitrogen or argon. Two different set-ups are assembled to test the charge–discharge cycling of the battery, H-cell and flow cell. The H-cell experiments are described in detail in the ESI.† 0.15–0.3 M $TEABF_4$ and 0.15–0.3 M $[Cu(CH_3CN)_4]BF_4$ in acetonitrile–propylene carbonate solutions were used as electrolytes in all experiments. Here, $TEABF_4$ was utilized to improve the conductivity of the electrolytes. The anion exchange membrane (FAB-PK-130, Fumatech) is either directly included under its dry state or soaked in acetonitrile with 0.15 M $TEABF_4$ for 24 hours before utilization. All gaskets, seals and tubing need to be chemically resistant to acetonitrile. For the flow cell, the usual stack is constructed with the anionic membrane and Ti current collectors. Copper foam (CU003841, Goodfellow, 6.35 mm thick, 16 pores per cm, 2 × 4 cm) and carbon-felt electrodes (SGL Carbon, 2 × 4 cm) were used for the negative and positive side, respectively. The membrane area of 8 cm^2 was used for normalization. The photo of the set-up is shown in the ESI.† The calculations of the coulombic and energy efficiencies are illustrated in the ESI.† Electrochemical impedance spectroscopy was utilized to evaluate the Ohmic resistance of the cell.

Cu-nanoslurry flow battery

Cu nanopowder solutions of 5 and 15 wt% were prepared with the supporting electrolyte. Carbon felt and reticulated vitreous carbon (ERG Aerospace, 6.35 mm thick, 16 pores per cm, 2 × 4 cm) electrodes were utilized for the positive and negative side, respectively. The slurry electrolyte tank was mixed to keep the copper in suspension.

Thermal regeneration

Two consecutive charge processes with thermal treatment are carried out to characterize the voltage, power and discharge that can be obtained during the discharge of the electrolyte in a RFB. During the first charge, the electrolyte (50% (vol/vol) ACN and PC, 0.3 $TEABF_4$, 0.15 M $[Cu(CH_3CH)_4]BF_4$) containing a Cu nanoslurry (15% (w/w)) is heated overnight between 120 and 140 °C to distillate the ACN from the solution and to produce the disproportionation of the Cu(I) to Cu and Cu(II). After this process, the Cu–Cu(II)-PC solution that remains after the distillation is centrifuged to separate the solid Cu (the slurry and reduced Cu(I)) from the Cu(II) solution. The ACN is introduced back into the Cu(II) solution and a part is kept to fluidize the Cu slurry and to allow the future oxidation of Cu to the Cu(I) complex $[Cu(CH_3CH)_4]BF_4$. The solutions of Cu and Cu(II) flow, respectively, in the RFB with an RVC-Ti current collector on the negative side and with a Ti current collector coupled with a C-felt electrode on the positive one. The discharge current is set to 10 mA cm^{-2}. When the electrolyte is discharged, both sides are mixed together in one tank and another heat treatment is applied. By following the same procedure as before, the electrolyte is again discharged in the RFB.

Results and discussion

Thermally regenerative copper battery

The operation of the copper battery is based on three oxidation states of copper, as illustrated in Scheme 1. Upon discharge, metallic copper is oxidized to Cu(I) on the negative electrode and Cu(II) is reduced to Cu(I) on the positive electrode.[31,41–44] Copper complexing agents such as acetonitrile, ammonia, or chloride are required to stabilize the Cu(I) oxidation state.[45–49] With acetonitrile or ammonia this property can be used for advantage to realize a thermally regenerative battery, as destabilization of the Cu(I) can be achieved in a thermal reaction simply by removing the acetonitrile into the gas phase upon distillation. Once the complexing agent is removed, Cu(I) disproportionates according to the following reaction: $2Cu(I) \rightarrow Cu + Cu(II)$, *i.e.* nucleation of Cu particles and generation of Cu(II) species dissolved in solution takes place. Obviously, a co-solvent such as water or propylene carbonate used in this work is required to avoid precipitation of Cu(II) salts. Solid Cu and the Cu(II) containing solution can be separated and introduced back into the battery after the addition of the recovered acetonitrile, finishing the thermal regeneration step. Now the energy is stored in the battery, and can be converted into electricity upon demand. Additionally, the battery can

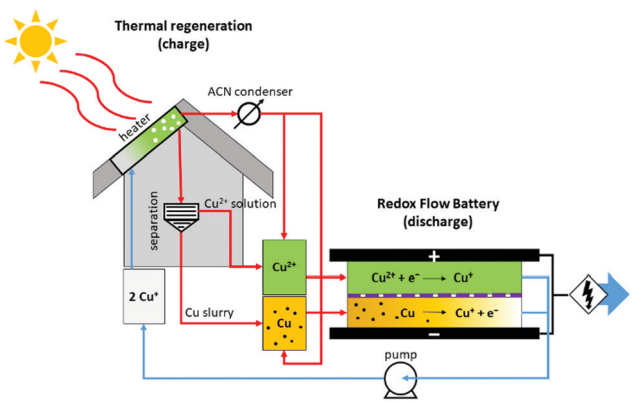

Scheme 1 Scheme of the cycle process of the Cu redox flow battery for heat to power conversion.

be charged with electricity (*vide infra*) instead of the thermal charge.

All copper redox flow battery

To understand how efficiently the chemical energy produced in the thermal step can be converted into electricity, experiments with the all-copper battery are required. The charge and discharge reactions of such a battery are shown below.

Negative electrode (Cu):

$$Cu^{+} + e^{-} \underset{\text{discharge}}{\overset{\text{charge}}{\rightleftharpoons}} Cu$$

Positive electrode (carbon felt):

$$Cu^{+} \underset{\text{discharge}}{\overset{\text{charge}}{\rightleftharpoons}} Cu^{2+} + e^{-}$$

The electrochemical kinetics of the negative electrode reaction has been investigated earlier,[50] and the study of the positive electrode reaction is included in the ESI.† In short, both reactions have reasonably facile kinetics, with much higher reaction rates than obtained in the state-of-the-art vanadium flow batteries.

In Fig. 1, charge–discharge cycles of the RFB with a 0.5 M $LiPF_6$ supporting electrolyte are shown, with improved efficiencies in comparison with the H-cell results included in the ESI.† The coulombic efficiency is stable during the battery test and its averaged value is 99% (Fig. 1b). However, the energy efficiency decreases with time, starting from 81% and reducing to 44% after 50 cycles (Fig. 1b). A similar trend is also observed for the state of charge (Fig. 1b) and is assigned to solvent crossover through the anionic membrane, which is observed as a significant change of the volume in both tanks (at the end of the cycling test: $V_{-} < V_{+}$). However, the state of charge and energy efficiency can be easily recovered if the discharge solutions (mainly Cu(I) species on both sides) are mixed and equally separated back between the positive and negative tanks (see the ESI† for more details). This behaviour is also observed in typical vanadium redox flow batteries, and electrolyte rebalancing systems have been developed to deal with this problem.[51–55]

The energy storage density of the described system is 2.6 W h L^{-1} (0.15 M Cu(I)-species), but could be increased by increasing the concentration of copper.[42]

Another approach is to replace the copper electrode with carbon foam and flow a slurry composed of copper nanoparticles on the negative side. This transforms the system to a true flow battery, where the capacity of the system is independent of the electrode mass and depends only on the volume of the electrolyte. Polarization curves with 5 wt% and 15 wt% nanoslurry electrolytes are shown in Fig. 1c, displaying even higher power densities than could be obtained with copper foam.

Thermal regeneration

The reaction leading to the formation of Cu(II) and Cu from Cu(I) is a disproportionation. The description of this process is given when Cu(I) complexes with acetonitrile are destabilized by heat:

$$2Cu(CH_3CN)_4^{+} \underset{\text{Under } N_2}{\overset{120-160\ ^{\circ}C}{\rightleftharpoons}} Cu + Cu^{2+} + 8CH_3CN$$

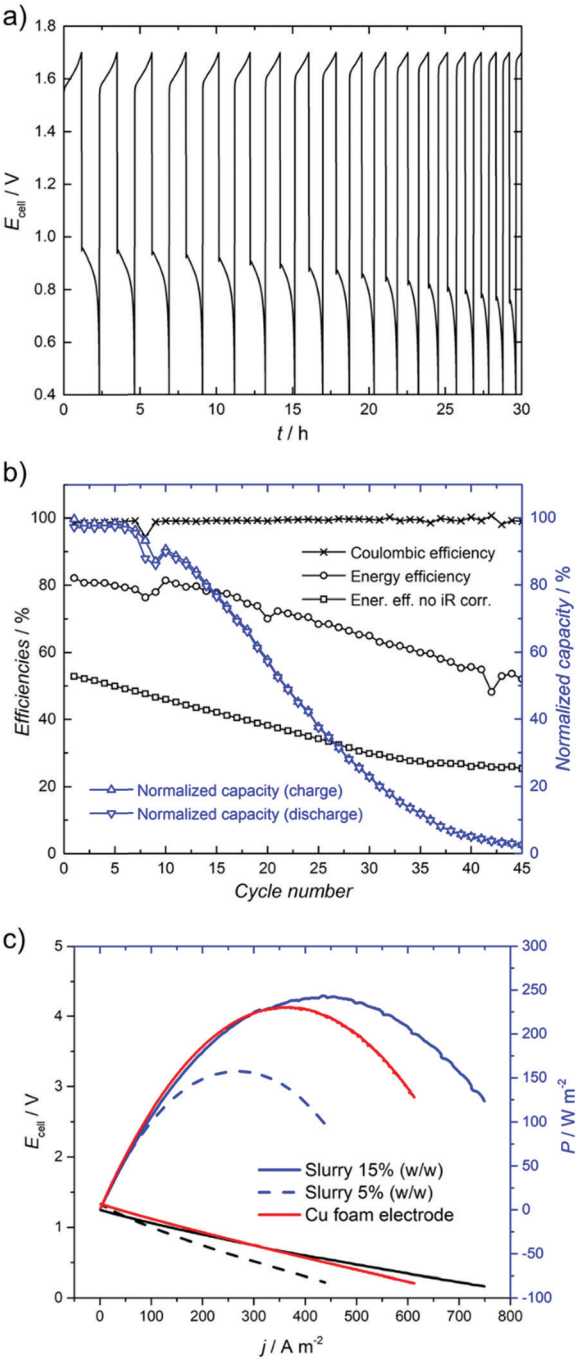

Fig. 1 Cu redox flow battery with $[Cu(CH_3CN)_4]PF_6$ (0.15 M) and $LiPF_6$ (0.5 M) and i = 10 mA cm^{-2}, (a) potential cycling (not *iR* corrected) with time and (b) efficiencies and normalized capacities of the battery for all cycles. The volume of both electrolytes was 25 mL. (c) Power output with Cu foam and nanoslurry electrolytes with a composition of 50 vol% ACN containing 0.15 M $[Cu(CH_3CN)_4]BF_4$, at the flow rate of 40–45 mL min^{-1}. The *iR* corrected data are shown in the ESI.†

Differential scanning calorimetry (DSC) measurements shown in the ESI,† demonstrate that the disproportionation step can be distinguished from the acetonitrile vaporization at 82 °C, taking place at *ca.* 160 °C for solid $Cu(CH_3CN)_4BF_4$. This indicates that the disproportionation reaction cannot simply be induced by the distillation of the acetonitrile solvent close to 81 °C, but a surplus of heat is required to destabilize the Cu(I) complex. Further investigations indicate that Cu(I) disproportionation could be realized at temperatures near 120 °C for a 30% acetonitrile–70% propylene carbonate solution. The thermodynamic parameters including enthalpies of vaporization and heat capacities for various ratios of Cu(I) containing acetonitrile–propylene carbonate mixtures have been measured with DSC, and are reported in the ESI.† These results also confirm that it is necessary to consider the excess energy of destabilizing the complex, as it is clearly not accurate to consider simple evaporation of the complexing agent as suggested previously.[21] This issue was also highlighted recently.[22]

The Cu(I) solution was heated under nitrogen at 120 °C to induce thermal regeneration. In order to keep a solution after the disproportionation, the solvent is partially composed of propylene carbonate, which remains in the liquid state (b.p. = 242 °C). The completion of the reaction and the formation of Cu particles and Cu(II) solution was confirmed by the colour transition from the transparent Cu(I) solution to the Cu(II) and with the appearance of some metallic Cu particles. We analysed the resulting solution with different techniques to verify and describe the presence of Cu(II) and metallic Cu. The acetonitrile condensate removed during thermal regeneration is collected to be introduced back in the system for the electrochemical discharge.

Dynamic light scattering (DLS) was used to analyse the size distribution of the thermally regenerated Cu particles, found to be between 70 and 460 nm in diameter, as shown in Fig. 2a. The average value for the diameter of the synthesised Cu particles is 187 ± 1 nm with a peak of population around 122 nm. TEM analysis shown in Fig. 2b indicates that smaller Cu particles down to 5 nm in diameter are also present. This implies that many different sizes of metallic Cu are produced during the thermal treatment of Cu(I). The complete conversion of Cu(I) to Cu and Cu(II) was confirmed by UV/Vis spectroscopy and bulk electrolysis, as shown in the ESI.†

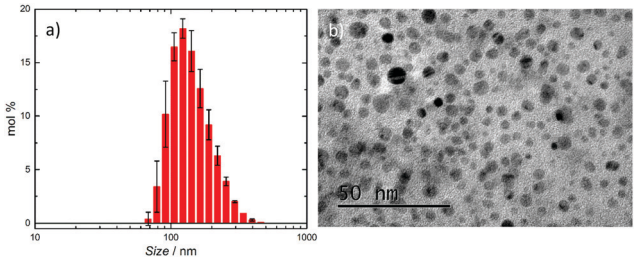

Fig. 2 After thermal regeneration from $[Cu(CH_3CN)_4]BF_4$, (a) Cu NP size distribution from DLS measurement and (b) TEM images of Cu particles produced upon thermal regeneration.

A flow cell was assembled to demonstrate that the system can be used to realize heat-to-power conversion. Four different methods were tested: (1) discharge of the positive side only, (2) 1st discharge of the full cell with nanoslurry electrolyte, (3) followed by a second cycle, and (4) discharge of the full cell, with Cu particles filtered off and added into the cell. In the first case copper particles were separated from the solution by filtration, and the recovered Cu(II) electrolyte was introduced into the positive side of the cell. A fraction of the distilled acetonitrile was introduced back in the Cu(II) solution to obtain the positive electrolyte, and copper foam was used as the negative electrode. In the fourth case the filter with Cu particles was introduced between the carbon foam current collector and the anionic membrane. In the second case, copper nanoslurry particles were separated by centrifugation. A large fraction (*ca.* 15 mL) of the recovered acetonitrile was added into the slurry, resulting in *ca.* 90% CH_3CN solution, and *ca.* 10 mL was added into the positive electrolyte (30% v/v CH_3CN). For the third case, discharged electrolyte from the first cycle was heat regenerated again, and the discharge was performed as during the first cycle.

The electrochemical discharge of the thermally charged battery at a constant current is shown in Fig. 3, and polarization curves in Fig. 4. When heat-regenerated solution was used on the positive side, with Cu foam as the negative electrode, the cell voltage is around 1 V and the capacity of the discharge corresponds to 85–90% of the theoretical capacity of the battery. This difference might come from the loss of some Cu(II) solution during the thermal regeneration process, but it could be also due to an incomplete thermal treatment of the initial Cu(I) solution. In this case the cell was limited by the Cu(II)/Cu(I) couple. For the last case, much lower discharge voltages and capacities are obtained, because also the negative electrode reaction limits the cell performance, and at some point contact between the Cu-particles and the electrode is lost. Higher discharge voltage and capacity is reached when 15 wt% Cu nanoslurry electrolyte is used in the second and third cases. The first cycle allowed utilization of 80% of the nominal capacity, while this number was reduced to 70% for the second discharge. Further cycling is required to evaluate the long term stability of the system, but the use of the nanoslurry electrode allows envisaging a full process based on this concept. These curves also prove that heat storage is possible inside a Cu RFB through a chemical energy conversion, with average power of 75 W m^{-2}.

The performance of the Cu-RFB is described in Fig. 4 by the power production for the three different cases. The highest power density of 200 W m^{-2} is achieved with a Cu-foam electrode, but a nanoslurry system is able to show power densities of *ca.* 150 W m^{-2}. These values compare favourably with the earlier report of 136 W m^{-2} for the aqueous ammonia based Cu-system,[21] and of 236 W m^{-2} for the same system at increased temperatures.[20] According to these results, the power that can be produced from a thermal treatment is promising and allows considering this Cu-RFB as a potentially efficient tool to convert heat into stored electricity. Furthermore, if the

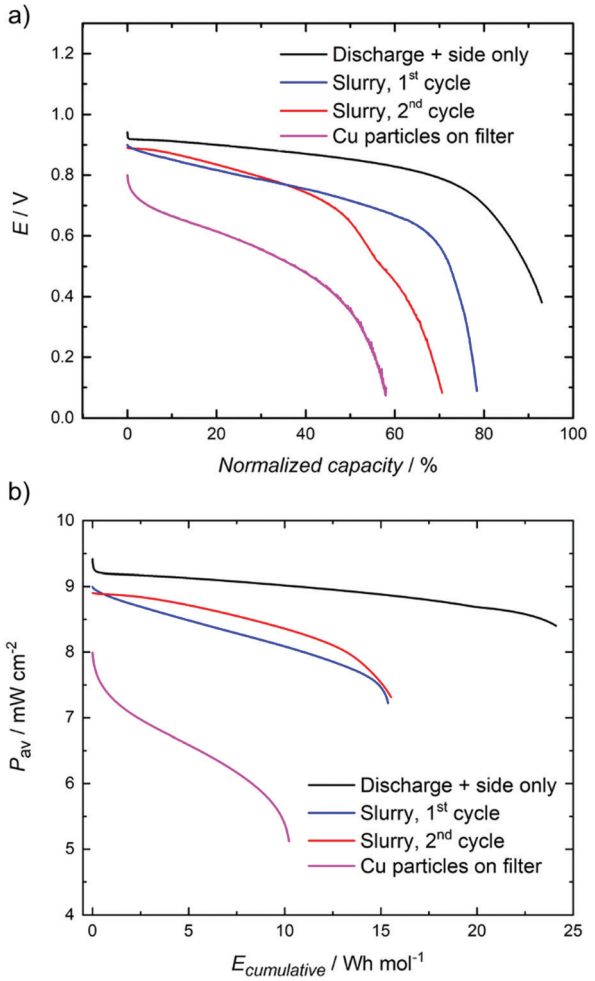

Fig. 3 (a) Discharge curves of the heat-regenerated RFB at 10 mA cm^{-2}. The positive electrolyte is composed of heat-regenerated $Cu(BF_4)_2$ (0.15 M) and $TEABF_4$ (0.15 M) in acetonitrile–propylene carbonate mixture and the negative electrolyte of $TEABF_4$ (0.15 M) in acetonitrile–propylene carbonate mixture. The acetonitrile is collected from the distilled fraction during the thermal disproportionation of the Cu(I). Additionally, on the negative side, the filter with the Cu particles is added in parallel to the membrane. Volumes of the electrolytes on the positive side are 20, 10, 10 and 8 mL, respectively. (b) Average power density output of the RFB during discharge *vs.* the cumulative energy output per mol of Cu^{2+}. Area of the membrane is 8 cm^2. The *iR* corrected data are shown in the ESI.†

resistance of the system could be decreased, much better performance could be obtained (see i*R*-corrected polarization and power curves in the ESI,† showing significant increase in power density). Such improvements are expected in the future, considering that the membranes developed for non-aqueous systems are inferior in comparison to the membranes used for aqueous systems.[56]

Thermodynamic analysis

When considering the thermal charging of the battery, disproportionation of Cu(I) requires higher temperatures of around 120–160 °C than the simple evaporation of acetonitrile, depending slightly on the acetonitrile–propylene carbonate ratios. We can determine the theoretical efficiency of the battery based on the values of the vaporization and reaction enthalpies and the heat capacity, as illustrated below. The efficiency is defined by the ratio of the output energy (electrical work) and the input heat, which is required for the vaporisation of acetonitrile, destabilization of Cu(I) and heating of the solution:

$$\eta = \frac{W_{\text{elec}}}{2Q_{\text{tot}}} = \frac{nFE_{\text{cell}}c_{[\text{Cu(I)(ACN)}_4]^+}}{2(Q_{\text{sol}} + Q_{\text{vap}} + Q_{\text{rxn}})}$$
$$= \frac{nFE_{\text{cell}}c_{[\text{Cu(I)(ACN)}_4]^+}}{2(\Delta T \times C_{\text{p}} \times c_{\text{tot}} + \Delta H_{\text{vap}}^{\text{ACN}} \times c_{\text{ACN}} + \Delta H_{\text{rxn}}^{\text{Cu(I)}} \times c_{[\text{Cu(I)(ACN)}_4]^+})} \quad (1)$$

where η is the theoretical efficiency, W_{elec} is the electrical work density extracted from the system, and Q_{tot} is the total amount of heat per volume required for the thermal regeneration. The factor 2 in the nominator is required because the combined electrolyte volume from both the negative and positive side needs to be heated. n = 1 is the number of electrons in the electrochemical reaction, F is the Faraday constant, E_{cell} is the cell voltage, and $c_{[\text{Cu(I)(ACN)}_4]^+}$ is the concentration of the Cu(I) species. Q_{tot} is composed of the heat required to heat the given volume of the solution to the hot temperature (Q_{sol}), the heat required to evaporate the free acetonitrile (Q_{vap}) and the heat required for the disproportionation reaction (Q_{rxn}). These values can be estimated when the difference between the hot and the cold temperature (ΔT), molar heat capacity of the whole solution (C_{p}) and the total concentration of all the species in the solution (including Cu-species, ANC and PC), molar heat of vaporisation of ACN ($\Delta H_{\text{vap}}^{\text{ACN}}$), acetonitrile concentration (c_{ACN}) and the disproportionation reaction enthalpy ($\Delta H_{\text{rxn}}^{\text{Cu(I)}}$) are known. All of these parameters have been measured for a number of different solution compositions, and the values are reported in the ESI.† For the demonstrated system, the theoretical efficiency for the heat-to-power conversion is 2.2%. The maximum efficiency of a work production by heat conversion is that of a Carnot cycle. With T_{cold} at 343 K and T_{hot} between 433 K, the maximum efficiency is 21%.

Envisaged improvements

The reported system shows low energy storage density of 2.6 W h L^{-1}. This is the theoretical value for the battery containing 0.15 M $[Cu(CH_3CN)_4]BF_4$ electrolyte. However, Li *et al.* have reported that the solubility of the $[Cu(CH_3CN)_4]^+$ salts in acetonitrile can be increased by a factor of 10 to 1.5 M by utilizing the TFSI-anion as a counter ion.[42] This system would show much improved energy storage density of 26 W h L^{-1}, although the solubility of the Cu^+ and Cu^{2+} salts in the presence of the co-solvent have to be confirmed. Additionally, the theoretical efficiencies for the heat to power conversion should also increase. As described in the ESI,† two main factors influencing the heat conversion efficiency are acetonitrile and Cu(I) concentrations in the electrolyte. With increasing amounts of acetonitrile, more heat is required for the distillation process and lower efficiencies are reached (2% for a 100% acetonitrile solution with 0.3 M $[Cu(CH_3CN)_4]BF_4$ against 5% for a 10% acetonitrile solution). An opposite effect is predicted according to the Cu(I) concentration with 13% for a 1.5 M

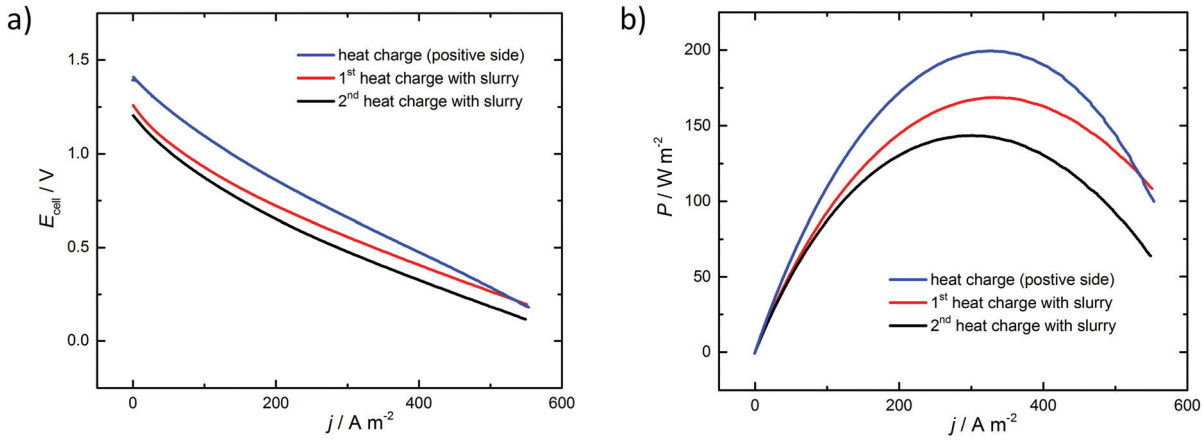

Fig. 4 (a) Polarization curves (no *iR* correction) and (b) corresponding power production of the Cu-RFB in different conditions. The starting solution for the thermal treatment of Cu(I) (0.3 M) to Cu–Cu(II) has a solvent composition of 50% acetonitrile in propylene carbonate. The polarization curves are done inside the cell with Cu foam electrode, named heat charge positive side (blue curve), inside a cell with Cu slurry electrode showing the first discharge (red curve) and second discharge (black curve) after two consecutive heat charge processes. The volume of the positive electrolyte was 20, 10 and 10 mL and the flow rate was 40–45 mL min^{-1}.

solution and 5% for a 0.3 M solution both containing 10% acetonitrile. Hence, for a battery with an optimized thermal energy conversion, low acetonitrile ratio and high Cu(I) concentration are preferable. Nevertheless, it is important to highlight that the voltage potential and kinetics parameters will decrease with decreasing acetonitrile content. Additionally, a significant amount of heat is required for heating up the solution. Therefore, co-solvent with lower heat capacity would improve the efficiency. Efficiencies approaching 65% of the Carnot efficiency for heat to power conversion (up to 13%) could be achieved with optimized solution compositions.

It is also worth noting that these values are theoretical efficiencies, calculated based on the measured or estimated thermodynamic properties. Therefore losses due to the pumping, overpotentials *etc.* are not included in this number. Commercial flow batteries are able to demonstrate stack level energy efficiencies of 70–80% depending on the discharge currents.[57] As this number takes into account the inefficiencies in both charging and discharging, the energy efficiency of the discharging step would be *ca.* 80–90%. Furthermore, about 5% of the energy in a typical flow battery is lost in pumping during discharge (2.5% loss assumed for both sides).[57] In this case the negative side is a slurry with twice the specific density of only the electrolyte. The viscosity is also significantly higher, up by a factor of 5 reported for carbon nanotube slurry.[36] Therefore the pump consumption of the negative side could be 25% of the discharge energy, while the number for the positive side would be 2.5% (this pumping loss may actually be an overestimation, as a recent paper suggests that pumping losses in a slurry system can be reduced to $<1\%$ of the energy output[58]). This would result in the heat-to-power conversion efficiencies of 8%. The total efficiency depends also on the energy required for separation of solid copper. Energy required by centrifugation could become unreasonable, so other more cost-effective methods such as hydrocyclones could be envisaged for solid–liquid separation.

We acknowledge that there are many uncertainties behind these assumptions. For example, it is questionable if the performance of the Cu flow battery will be able to match the performance of the vanadium system. Also, the effect of the increased viscosity for the pump power consumption would require more detailed studies. In the present system the nano-slurry is flowing through a porous electrode, resulting in significant pressure losses. This geometry should be optimized to realize a system with the best performance, both in terms of fluid flow and electrochemical performance. Additionally, open questions

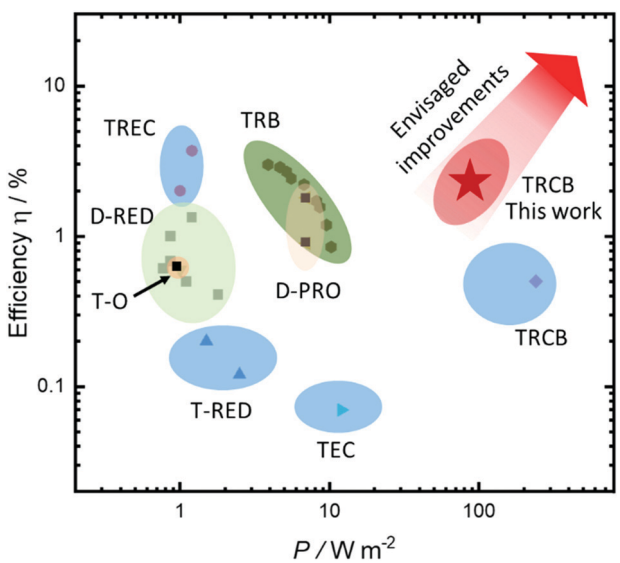

Fig. 5 Energy efficiency and power density of recent methods reported in the literature. Data and detailed evaluation of the other techniques are provided in ref. 19. D-PRO, distillation-pressure-retarded osmosis; D-RED, distillation-reverse electrodialysis; TEC, thermoelectrochemical cells; T-O, thermo-osmosis; TRCB, thermally regenerable complexation-based battery; TREC, thermally regenerative electrochemical cycle; T-RED, thermolysis-reverse electrodialysis; TRB, thermally regenerative batteries.

include what the efficiency of the thermal regeneration step is, and how much energy the solid/liquid separation will take.

A further challenge is to match the timescale of the discharge and thermal charge, as thermal charge appears to take considerably more time than electrochemical discharge. There are two options, batch-wise operation where thermal charge is realized independently of the discharge, or continuous operation. In batch-wise operation heat is utilized only occasionally, resulting in non-optimal utilization of heat and variable power output, although these effects could be minimized by incorporating heat storage into the system. Continuous operation would require larger volume of the liquids due to the hold-up in the heat regeneration step, but steady power output would be possible.

Comparison of the current system with recent techniques proposed in the literature in terms of efficiency and power density is given in Fig. 5. Our system has now demonstrated a theoretical efficiency of 2.2% at the average power of 75 W m^{-2} and maximum power density of 150 W m^{-2}. We believe that increasing the concentration of the copper salt would allow increasing the efficiency close to 10% while also increasing the power density.

Conclusions

In this paper, we present thermally regenerative non-aqueous copper batteries as a means to convert low-grade thermal energy into electrical energy, stored in a battery. We have investigated the electrochemistry and the thermodynamic properties of the system, and show that heat of *ca.* 120 °C temperature can be converted into electricity. Replacement of water with a higher boiling point co-solvent, propylene carbonate, allows unprecedented cell voltages and high output power for a thermo-electrochemical battery. The applicability of the nanoslurry electrode for the negative side of the battery is also demonstrated, allowing multiple cycles of heat-to-power conversion.

Overall, this work opens the way to thermo-electrochemical electricity generation to exploit industrial waste heat and thereby provide new alternative routes of renewable energy generation.

Conflicts of interest

There are no conflicts to declare.

Acknowledgements

This work was supported by the financial fund from the Swiss National Science Foundation under Grant Ambizione Energy 160553. P. P. gratefully acknowledges the Academy Research Fellow funding from the Academy of Finland (Grant number 315739). The authors thank Dr Véronique Amstutz for her help with the SEM/TEM imaging and Thierry Udrisard for the access to the DSC machine of the HES Sion. Dr Heron Vrubel, Patrick Favre, Stephane Voeffray and Robin Délèze are acknowledged for their help with the motorized set-up for Cu particle production by a cathodic corrosion method. The authors are also grateful to Michèle Raymond for the design of the scheme illustrating the heat regeneration system, and for Prof. Jose Manzanares (University of Valencia, Spain) for fruitful discussion regarding thermodynamics of these systems.

Notes and references

1 I. Johnson, W. T. Choate and A. Davidson, *Waste Heat Recovery: Technology and Opportunities in U.S. Industry*, BCS Incorporated, 2008.
2 A. Waske, D. Dzekan, K. Sellschopp, D. Berger, A. Stork, K. Nielsch and S. Fähler, *Nat. Energy*, 2019, **4**, 68.
3 A. P. Straub, N. Y. Yip, S. Lin, J. Lee and M. Elimelech, *Nat. Energy*, 2016, **1**, 16090.
4 A. M. Rowe, *Nat. Energy*, 2019, **4**, 12.
5 M. Rahimi, A. P. Straub, F. Zhang, X. Zhu, M. Elimelech, C. A. Gorski and B. E. Logan, *Energy Environ. Sci.*, 2018, **11**, 276–285.
6 D. Champier, *Energy Convers. Manage.*, 2017, **140**, 167–181.
7 M. Hamid Elsheikh, D. A. Shnawah, M. F. M. Sabri, S. B. M. Said, M. Haji Hassan, M. B. Ali Bashir and M. Mohamad, *Renewable Sustainable Energy Rev.*, 2014, **30**, 337–355.
8 X. F. Zheng, C. X. Liu, Y. Y. Yan and Q. Wang, *Renewable Sustainable Energy Rev.*, 2014, **32**, 486–503.
9 D. Y. Goswami and F. Kreith, *Energy Conversion*, CRC Press, 2007.
10 J. Bao and L. Zhao, *Renewable Sustainable Energy Rev.*, 2013, **24**, 325–342.
11 A. B. Little and S. Garimella, *Energy*, 2011, **36**, 4492–4504.
12 A. I. Kalina, *J. Eng. Gas Turbines Power*, 1984, **106**, 737–742.
13 S. Ogriseck, *Appl. Therm. Eng.*, 2009, **29**, 2843–2848.
14 M. F. Dupont, D. R. MacFarlane and J. M. Pringle, *Chem. Commun.*, 2017, **53**, 6288–6302.
15 M. Jokinen, J. A. Manzanares, K. Kontturi and L. Murtomäki, *J. Membr. Sci.*, 2016, **499**, 234–244.
16 D. Reynard, C. R. Dennison, A. Battistel and H. H. Girault, *J. Power Sources*, 2018, **390**, 30–37.
17 C. Gao, S. W. Lee and Y. Yang, *ACS Energy Lett.*, 2017, **2**, 2326–2334.
18 N. Y. Yip, D. Brogioli, H. V. M. Hamelers and K. Nijmeijer, *Environ. Sci. Technol.*, 2016, **50**, 12072–12094.
19 I. Facchinetti, R. Ruffo, F. La Mantia and D. Brogioli, *Cell. Rep. Phys. Sci.*, 2020, 100056.
20 F. Zhang, N. LaBarge, W. Yang, J. Liu and B. E. Logan, *ChemSusChem*, 2015, **8**, 1043–1048.
21 F. Zhang, J. Liu, W. Yang and B. E. Logan, *Energy Environ. Sci.*, 2015, **8**, 343–349.
22 F. Vicari, A. D'Angelo, Y. Kouko, A. Loffredi, A. Galia and O. Scialdone, *J. Appl. Electrochem.*, 2018, **48**, 1381–1388.
23 M. Rahimi, T. Kim, C. A. Gorski and B. E. Logan, *J. Power Sources*, 2018, **373**, 95–102.
24 P. Peljo, D. Lloyd, N. Doan, M. Majaneva and K. Kontturi, *Phys. Chem. Chem. Phys.*, 2014, **16**, 2831–2835.
25 A. J. Parker, D. M. Muir, Y. C. Smart and J. Avraamides, *Hydrometallurgy*, 1981, **7**, 213–233.
26 W. Wang, H. Tian, G. Shu, D. Huo, F. Zhang and X. Zhu, *J. Mater. Chem. A*, 2019, **7**, 5991–6000.

27 M. Marino, L. Misuri, A. Carati and D. Brogioli, *Energies*, 2014, **7**, 3664–3683.
28 D. Brogioli and F. L. Mantia, *AIChE J.*, 2019, **65**, 980–991.
29 D. Brogioli, F. La Mantia and N. Y. Yip, *Renewable Energy*, 2019, **133**, 1034–1045.
30 D. Brogioli, F. La Mantia and N. Y. Yip, *Desalination*, 2018, **428**, 29–39.
31 B. Kratochvil and K. R. Betty, *J. Electrochem. Soc.*, 1974, **121**, 851–854.
32 T. J. Petek, N. C. Hoyt, R. F. Savinell and J. S. Wainright, *J. Power Sources*, 2015, **294**, 620–626.
33 W. Yan, C. Wang, J. Tian, G. Zhu, L. Ma, Y. Wang, R. Chen, Y. Hu, L. Wang, T. Chen, J. Ma and Z. Jin, *Nat. Commun.*, 2019, **10**, 1–11.
34 Z. Qi and G. M. Koenig, *J. Vac. Sci. Technol., B*, 2017, **35**, 040801.
35 H. H. Morgan, *J. Chem. Soc., Trans.*, 1923, **123**, 2901–2907.
36 B. J. Hathaway, D. G. Holah and J. D. Postlethwaite, *J. Chem. Soc.*, 1961, 3215–3218.
37 B. J. Hathaway, D. G. Holah and A. E. Underhill, *J. Chem. Soc.*, 1962, 2444–2448.
38 G. J. Kubas, B. Monzyk and A. L. Crumbliss, in *Inorganic Syntheses*, ed. D. F. Shriver, John Wiley & Sons, Inc., 1979, pp. 90–92.
39 A. I. Yanson, P. Rodriguez, N. Garcia-Araez, R. V. Mom, F. D. Tichelaar and M. T. M. Koper, *Angew. Chem.*, 2011, **50**, 6346–6350.
40 J. Feng, D. Chen, A. S. Sediq, S. Romeijn, F. D. Tichelaar, W. Jiskoot, J. Yang and M. T. M. Koper, *ACS Appl. Mater. Interfaces*, 2018, **10**, 9532–9540.
41 E. A. Stricker, K. W. Krueger, R. F. Savinell and J. S. Wainright, *J. Electrochem. Soc.*, 2018, **165**, A1797–A1804.
42 Y. Li, J. Sniekers, J. Malaquias, X. Li, S. Schaltin, L. Stappers, K. Binnemans, J. Fransaer and I. F. J. Vankelecom, *Electrochim. Acta*, 2017, **236**, 116–121.
43 L. Sanz, D. Lloyd, E. Magdalena, J. Palma and K. Kontturi, *J. Power Sources*, 2014, **268**, 121–128.
44 D. Lloyd, E. Magdalena, L. Sanz, L. Murtomäki and K. Kontturi, *J. Power Sources*, 2015, **292**, 87–94.
45 M. A. Rizvi, S. A. Akhoon, S. R. Maqsood and G. M. Peerzada, *J. Anal. Chem.*, 2015, **70**, 633–638.
46 J. Torras and C. Alemán, *J. Phys. Chem. B*, 2013, **117**, 10513–10522.
47 J. Brugger, B. Etschmann, W. Liu, D. Testemale, J. L. Hazemann, H. Emerich, W. van Beek and O. Proux, *Geochim. Cosmochim. Acta*, 2007, **71**, 4920–4941.
48 L. Sanz, J. Palma, E. García-Quismondo and M. Anderson, *J. Power Sources*, 2013, **224**, 278–284.
49 D. B. Rorabacher, *Chem. Rev.*, 2004, **104**, 651–698.
50 I. Atek, S. Maye, H. H. Girault, A. M. Affoune and P. Peljo, *J. Electroanal. Chem.*, 2018, **818**, 35–43.
51 *US Pat.*, US6764789B1, 2004.
52 S. Corcuera and M. Skyllas-Kazacos, *Eur. Chem. Bull.*, 2012, **1**, 511–519.
53 K. Wang, L. Liu, J. Xi, Z. Wu and X. Qiu, *J. Power Sources*, 2017, **338**, 17–25.
54 A. Bhattarai, P. C. Ghimire, A. Whitehead, R. Schweiss, G. G. Scherer, N. Wai and H. H. Hng, *Batteries*, 2018, **4**, 48.
55 A. Bhattarai, N. Wai, R. Schweiss, A. Whitehead, G. G. Scherer, P. C. Ghimire, T. M. Lim and H. H. Hng, *Appl. Energy*, 2019, **236**, 437–443.
56 S.-H. Shin, S.-H. Yun and S.-H. Moon, *RSC Adv.*, 2013, **3**, 9095–9116.
57 D. Bryans, V. Amstutz, H. H. Girault and L. E. A. Berlouis, *Batteries*, 2018, **4**, 54.
58 Y. Zhu, T. Malai Narayanan, M. Tułodziecki, H. Sanchez-Casalongue, Q. Horn, L. Meda, Y. Yu, J. Sun, T. Regier, G. H. McKinley and Y. Shao-Horn, *Sustainable Energy Fuels*, 2020, DOI: 10.1039/D0SE00675K.